Efficient Fault Diagnosis of Squirrel Cage Induction Motors in Industrial Applications Using an CNN-LSTM Approach

Ulaganathan Jayapal*[ID], Sadyojatha Kalapur Mutt[ID]

Department of Electronics and Communication Engineering, Ballari Institute of Technology and Management, Ballari, Affiliated to Visvesvaraya Technological University, Belagavi 590018, India

Corresponding Author Email: ulaganathan@bitm.edu.in

ABSTRACT

This paper presents a Convolution Neural Network-Long Short Term Memory (CNN-LSTM) network architecture technique for defect diagnosis of squirrel cage induction motors. The CNN-LSTM strategy uses LSTM's ability to represent sequential data and CNN's ability to extract spatial features. The process involves gathering and preprocessing motor sensor data, processing it as 1D representations, and extracting spatial characteristics. CNN layers identify patterns in the data, while an LSTM network captures dependencies temporarily within feature sequences. The CNN-LSTM model classifies motor condition into fault categories or normal functioning. Extensive experimentation is conducted for assessing effectiveness of the CNN-LSTM technique, with the accuracy highest of 90.6% compared with technique existing. This method provides a reliable and effective method for defect diagnosis in industrial applications.

1. INTRODUCTION

Nikola Tesla and Galileo Ferraris contributed to the development of squirrel-cage induction motors in the late 19th century, marking a turning point in electrical engineering. These motors, patented in 1888, were crucial in the Second Industrial Revolution, supplying energy to machinery like conveyor belts and pumps [1]. Their simplicity, dependability, and efficiency influenced automation and factory productivity [2]. The motors' operations rely on electromagnetic induction principles and are used in different applications of industries, which include pumps, conveyor belts, and manufacturing equipment.

Squirrel cage induction motors are increasingly used in industrial settings due to their durability, high starting torque, and resilience in harsh industrial environments [3]. Essential in production line elements, petrochemical, mining, Heating, Ventilation, and Air Conditioning (HVAC), irrigation systems, water treatment plants, and electric trains and trams. However, they are susceptible to defects due to factors like vibration, temperature, current, acoustic noise, speed, voltage, and humidity [4]. To ensure their longevity, proactive monitoring, routine maintenance, and environmental considerations are crucial [5]. In recent years, deep learning-based fault identification has become an exciting field of study. Because of its complex structure, the deep learning (DL) algorithm can understand a wide data range associated with various levels of abstraction [6]. By independently extracting several signal features from, deep learning overcomes the difficulties of ML classifiers. Convolution Neural Network (CNN), deep neural networks, recurrent neural networks (RNN), deep Boltzmann machines, and stacked auto encoders (SAE) are DL methods examples. In fields like pattern recognition, human language understanding, picture analysis, and machine malfunction detection, DL has made major commitments [7]. Researchers in reference [8] have looked into the usage of STFT and deep learning to bearing defect diagnosis. A one-dimensional CNN algorithm is been suggested by researchers [9] for the identification of mechanical faults. A deep CNN algorithm is been used for identifying problems based on images created from unprocessed data using time-frequency representation [10].

Lee et al. [11] have used the CNN network for detecting broken bars and bearing problems. A number of deep learning techniques, which include DBM, SAE, and Deep Boltzmann Machine, are used to detect bearing failures. The authors in their work have published a CNN framework for identifying bearing defects using the envelope ordering spectrum from vibration signals [12]. Pandarakone et al. [13] suggested an anomaly diagnosis method using CNN and the Fast Fourier Transformation to detect bearing issues in induction motors. The authors proposed a CNN and inductive Wavelet transform method for detecting induction motor bearing failure [14]. In order to investigate the identification of bearing irregularities, Li et al. [15] employed a CNN model, the rapid Fourier Transformation analysis of vibration, and the root mean square results from the rapid Fourier transform computation.

Scientists examined the utilization of the CNN network and STFT of signals from vibration for fault identification in machines [16]. An approach for categorizing mechanical breakdowns utilizing CNN-based hidden Markov models was put out by Wang et al. [17]. Researchers suggested a hierarchical CNN to recognize various rolling bearings failure conditions [18]. With the aid of a hierarchical adaptable The

CNN network approach, Guo et al. [19] have proposed a bearing anomaly identification methodology.

Because of their ease of use and interpretability, traditional diagnostic techniques like the Fast Fourier Transform (FFT), Short-Time Fourier Transform (STFT), and Support Vector Machines (SVM) algorithms were used in the identification of motor faults. While STFT gives restricted time-frequency resolution because of its set window size, FFT delivers frequency-domain analysis but lacks temporal localization. Without domain-specific feature engineering, SVMs have trouble capturing complicated feature interactions, despite their effectiveness in linear separability [20].

On another hand, due to automatically extract abstract and hierarchical features from unprocessed sensor data from deep learning methods, they provide notable performance gains, especially when it comes to CNNs and RNNs. For instance, a comparison study by the researchers in their work, showed that a CNN model obtained over 96% accuracy on the same dataset, whereas SVM only achieved 85% classification accuracy in noisy settings [21]. Similarly, STFT-based techniques demonstrated a 78% detection rate under varied load conditions, whereas Long Short-Term Memory (LSTM) networks attained an accuracy of up to 94%. The better defect recognition capabilities, and resilience are amply demonstrated by these quantifiable differences, particularly when included with Industrial IoT (IIoT) frameworks. Table 1 represents the comparison of various motor fault detection methods.

Table 1. Quantitative comparison of traditional diagnostic methods and learning techniques for fault detection of motor [21]

Method	Accuracy under Noise	Accuracy under Load Variation	Feature Engineering Required
FFT	~75%	~68%	Yes
STFT	~78%	~72%	Yes
SVM	~85%	~80%	Yes
CNN	~96%	~92%	No
LSTM	~94%	~90%	No

The study proposes a hybrid method combining LSTM networks and CNNs to accurately diagnose faults in induction motors. The method unifies multi-modal sensor data, including vibration, temperature, current, sound, speed, and voltage measurements, allowing for a comprehensive examination of motor health. The CNN-LSTM model can identify defects early, allowing for preventative maintenance procedures. This innovative approach improves equipment performance and reduces downtime, making it a valuable tool for industrial machinery maintenance and defect finding.

2. LITERATURE WORK

This study proposes a hybrid CNN-MLPAM model for identifying motor malfunctions using multiple sensors. It uses attention mechanisms and Fast Fourier Transform to analyze signals, identifying essential information through sound features and time-frequency images. The model outperforms traditional vibration-based approaches, but lacks exploration of fault mechanisms [21].

The study focuses on detecting and isolating stator and rotor winding issues in squirrel-cage induction motor structures,

improving the security and reliability of China Railway High-speed trains.

This research proposes a technique to analyze motor current data for diagnosing bearing issues in induction motors. Using statistical attributes, genetic algorithms, and machine learning models, the technique improves accuracy and simplifies computation. The results show that the proposed approach is suitable for fault diagnosis in IM bearings, requiring more information than direct signals [22].

This article uses machine learning to identify demagnetization faults in PMSM drive systems, analyzing frequency and time components using STFT. It compares k-nearest neighbors and multilayer perceptron models, focusing on individual elements' impact on model performance [23].

This study proposes a novel approach for detecting and diagnosing issues in permanent magnet synchronous motors (PMSM) using stator phase currents. It integrates VMD, Hilbert-Huang transform, and a convolutional neural network to analyze current signals, detect faults, and classify motor malfunctions [24].

This article recommends using a one-dimensional convolutional neural network for detecting motor malfunctions in PMSM. This model uses weak supervision and features to assess motor strength and electrical signals, identifying causes of issues like speed, load variations, and eccentricity. The approach outperforms traditional machine learning techniques but has significant costs [25].

3. PROBLEM STATEMENT

The complex issue of guaranteeing the steady and effective performance of squirrel cage induction motors in the diverse range of industrial applications is the current problem [26]. In industrial operations, motors are essential, but flaws such electrical anomalies, unbalance, and bearing wear can result in expensive downtime, equipment damage, and production delays [27]. With an emphasis on precise problem identification and early fault detection, this project attempts to create an advanced defect detection system for industrial squirrel cage induction motors. It places a strong emphasis on upholding operational uptime, cutting maintenance expenses, and real-time monitoring.

In order to identify more serious issues, the system analyzes sensor data both geographically and temporally using CNNs and LSTM networks. It is resilient, able to handle noise and disruptions in industrial settings, and adjustable to different motor types and configurations. The optimal utilization of sensor data, which is routed through the neural network architecture for the optimum feature extraction and sequence modeling, is essential to the system's success in the search for data-driven insights. Computational efficiency is a critical component that guarantees the system can manage the continuous deluge of data generated by the requirements of real-time monitoring without putting undue strain on its processing capacity. Ultimately, the primary goal is simple: to create a fault detection system that is excellent at accurately identifying and classifying motor faults while simultaneously giving industrial operators timely and practical insights. This technology serves as a sentinel in the ever-evolving realm of industrial applications, guaranteeing the lifetime, dependability, and efficiency of squirrel cage induction motors. Its success could lead to enhanced production processes, cost savings, and increased industrial resilience in

the face of complex and dynamic difficulties in the industrial process.

4. OUTLINE OF THE PROPOSED MECHANISM

The suggested methodology is a systematic and meticulously planned process for the efficient fault diagnosis of squirrel cage induction motors in industrial applications using a CNN-LSTM approach. It begins with the gathering of sensor data from these important motors in industrial settings, which includes measurements of vibration, voltage, current, and temperature. Following the addition of annotations, this data is further enhanced, allowing for the classification of various motor running conditions, including both normal states and numerous fault scenarios, such as bearing wear, imbalance, and electrical anomalies. The innovative application of Convolutional Neural Networks (CNNs) for spatial feature extraction forms the basis of the methodology. The sensor data is processed as 1D representations in this stage, similar to spectrograms or time-domain signal profiles, enabling the CNN to independently identify and extract useful spatial characteristics from the information. After doing a geographic analysis, the task is handed off to LSTM networks, which are built to understand temporal connections within spatial feature sequences.
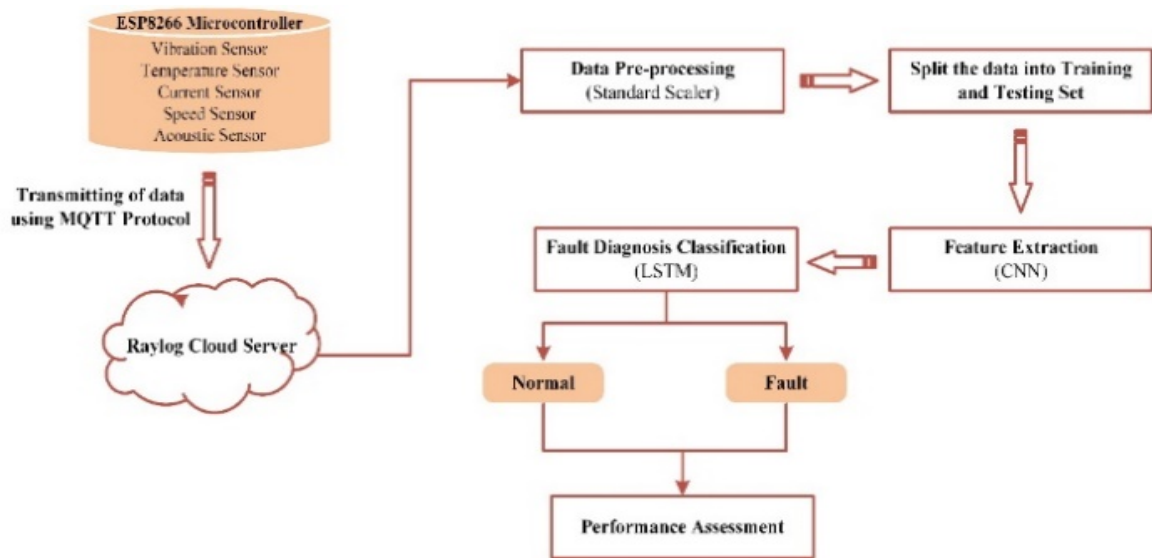

Figure 1. MQTT-based IIoT communication architecture for predictive motor maintenance

The suggested system's process is depicted in Figure 1. The next phases involve the training and validation of the model, which requires splitting the dataset into discrete sets. The training set is used to meticulously train the CNN-LSTM model, and continuous validation ensures that the hyper parameters are changed as necessary. Depending on the particular diagnostic goal, either a classification layer that allows for the multi-class classification of motor states or an anomaly detection layer that allows for the identification of deviations from conventional operational behavior complete the model design. Throughout the evaluation process, the model's performance is carefully assessed using metrics such as accuracy, precision, recall, and area under the ROC curve (AUC) to ascertain its effectiveness. Motivated by the influx of fresh data, a monthly maintenance and retraining program is implemented to sustain the model's ongoing effectiveness. This iterative process guarantees that the model may be modified to adapt to evolving motor conditions, enhancing motor dependability, reducing downtime, and simplifying industrial processes. This proposed methodology offers a thorough and efficient solution for industrial applications by utilizing the complementary strengths of CNNs and LSTMs to tackle the challenging issue of defect detection in squirrel cage induction motors.

4.1 Data collection and transmission

The ESP8266 microcontroller module was used to collect and analyze data from squirrel cage motor sensors, including vibration, temperature, current, acoustics, speed, voltage, and humidity. This extensive sensor data was efficiently and effectively transmitted according to the chosen communication protocol, MQTT, making sure it arrived at its destination safely and in real-time. Once transferred, the data was safely housed on the Raylog Cloud platform. It is present here pending additional examination and interpretation. This collection of sensor data is a useful tool for in-depth research and understanding of the motor's operation. Engineers and analysts can gain access to a plethora of knowledge by utilising the data kept on the Raylog Cloud, allowing them to forecast probable defects, improve overall reliability, and optimise the motor's performance. 1000 labeled samples representing a range of motor operating conditions, including both normal and fault scenarios (e.g., bearing defects, unbalance, misalignment) comprise the dataset used for this study. Sensors that measured vibration, temperature, current, voltage, speed, humidity, and acoustic signals were used to gather the data.

The dataset was divided as follows for the purpose of developing the model:
- 700 training samples (70%)
- For validation, 150 samples (15%)
- For testing, 150 samples (15%)

In order to evaluate the model's generalization performance, this division made sure it was trained efficiently and tested on unseen data. Despite its small size, the dataset is used as a controlled experimental benchmark to verify the CNN-LSTM framework that has been suggested for predictive motor fault

detection. Table 2 shows 10 sample datasets with several motor conditions-related metrics.

Table 2. Data description

Label	Vibration	Temperature	Current	Acoustic	Speed	Voltage	Humidity	Condition
0	1.26	60	19.01	69	1468	385	59	Normal
1	2.98	61	19.78	69	1542	405	52	Normal
2	3.40	63	20.84	66	1438	402	58	Fault
3	3.57	77	19.01	66	1497	383	60	Normal
4	5.18	71	21.10	62	1474	395	52	Fault
5	1.84	59	18.50	70	1475	388	55	Normal
6	4.22	72	21.42	67	1428	397	60	Fault
7	3.01	69	20.01	65	1459	390	57	Fault
8	1.92	60	18.84	68	1490	386	56	Normal
9	5.09	75	22.05	63	1410	398	61	Fault

4.1.1 MQTT-based communication architecture

Because of its lightweight architecture and applicability for real-time industrial applications, the Message Queuing Telemetry Transport (MQTT) protocol is used in the proposed IIoT system.

In the publish-subscribe architecture of the system, edge sensor nodes act as MQTT clients, transmitting motor condition parameters (e.g., vibration, temperature, current, acoustics, speed, voltage, and humidity) to a MQTT broker. The broker is hosted on either a local edge server or cloud-based solutions such as Raylog Cloud.

Each sensor node is connected to an ESP8266 microcontroller, which gathers sensor data and publishes it to certain MQTT topics. The subscriber modules, which consist of an edge analytics engine and a cloud-based deep learning inference system, receive this data in real time. This architecture supports Quality of Service (QoS) level 1, which ensures at-least-once message delivery, improving reliability in noisy industrial environments.

4.1.2 Preprocessing of data

Z-score data normalization is a crucial preprocessing technique used on squirrel cage motor sensor data to provide uniformity and comparability to the diverse range of sensor readings. The effective processing and use of data from multiple sensors, such as vibration, temperature, and current, are made possible by this technology. First, the mean and standard deviation are computed for every sensor variable throughout the whole dataset. Z-scores are then computed for each individual data point by deducting the mean and dividing by the standard deviation. The Z-scores that are produced display the standard deviation of a data point's distance from the mean. The data distribution is essentially reshaped by this transformation, which centers it around a mean of 0 and scales it to have a standard deviation of 1. The following equation determines the Z-score (Z) for a given data point (X):

$$Z = \frac{X - \mu}{\sigma} \tag{1}$$

where, μ is the standard deviation from the mean and is the mean (average); σ is the standard scores (also known as z scores) of the samples. The analysis is initially prevented from being dominated by variables with greater numerical ranges by removing discrepancies in characteristic scales. Furthermore, Z-scores could be utilised to evaluate the standard deviations by which each data point deviates from the mean. Understanding the meaning of sensor readings is made much easier with the help of this knowledge. In conclusion, Z-score normalisation opens the door for thorough and perceptive analysis of squirrel cage motor sensor data, facilitating industrial tasks including fault identification, proactive maintenance, and performance enhancement.

To guarantee data quality and model reliability, the preprocessing pipeline consists of a number of crucial steps in addition to Z-score normalization, which centers and scales the input features to standardize them.

Denoising: Because of mechanical disruptions or electromagnetic interference, sensor signals—particularly vibration and acoustic data—frequently contains high-frequency noise. This was lessened by applying a low-pass Butterworth filter, which eliminated noise above 100 Hz without changing the pertinent fault signatures.

Sampling rate alignment: To guarantee temporal synchronization, all signals were resampled to a consistent rate of 1 kHz because various sensors (such as temperature, current, and acoustic) function at various sampling frequencies. For precise multimodal feature fusion, particularly in time-series models like LSTM, this alignment is essential.

Outlier handling: To maintain continuity without skewing the model, data points that deviated more than three standard deviations from the mean were identified as possible outliers and handled via interpolation.

These preprocessing enhancements increase the CNN-LSTM architecture's input quality and enable reliable feature extraction from noisy industrial settings. Sensor data is transmitted at speeds optimized for accuracy and bandwidth:

Vibration and current: once every second.

Temperature: once every 5 seconds.

This design provides the best possible balance between energy consumption, bandwidth efficiency, and responsiveness, especially when wireless connectivity is implemented. The capability of the MQTT broker to buffer messages during short-term network failures adds robustness.

4.1.3 Actual deployment configuration

The proposed architecture was tested on a three-phase squirrel cage induction motor under different mechanical stress conditions. Temperature sensors (Resistance Temperature Detector), vibration sensors (MEMS-based), ultrasonic sensors (Acoustic), and current transducers (Hall Effect) were all interfaced with the ESP8266 module. These sensor nodes used a Wi-Fi-based MQTT network to transmit data to the Raylog cloud. The average end-to-end communication delay was found to be less than 100 milliseconds, and more than 97% of messages were sent in real time. The implementation verified the system's ability to deliver real-time problem identification and fast fault

notifications under a range of operational situations.

4.2 Convolutional neural network based feature extraction

CNNs revolutionize computer vision and image analysis by mimicking human visual system's ability to identify patterns, objects, and features in images [28]. This study explores the complex operations and significant consequences of CNNs in various fields such as image classification, object identification, facial recognition, medical image analysis, and autonomous vehicle navigation [29]. CNNs are powerful tools for studying time series data, aiding in finance, speech recognition, and healthcare, and can be enhanced with hybrid designs.

Squirrel cage induction motor fault diagnosis using CNNs prevents costly breakdowns and production downtime, improving operational effectiveness and motor longevity [30].

In order to effectively extract spatial and temporal features from multivariate sensor data, the CNN-LSTM model was proposed. As the first feature extractors, the convolutional layers employ 64 filters with kernel size 3 and stride 1 in the first layer, and 128 filters in the second layer, both of which have kernel size 3 and stride 1. In both layers, the ReLU activation function is utilized. To minimize spatial dimensions and manage overfitting, a max pooling layer is used, with a pool size of two and a stride of two. To improve generalization, the CNN block's output is sent to an LSTM layer made up of 100 units with a 0.2 dropout rate. For the purpose of temporal learning, the LSTM layer is set up to return sequences. A fully connected dense layer with 64 neurons that have been activated by ReLU comes next, followed by a final softmax output layer with two units that represent fault and normal conditions. Grid search was used to optimize hyper-parameters in order to balance the small dataset size with model complexity.

4.3 Long Short-Term Memory

A network structure called long short - term was created to address the persistent issues with gradients explosion and gradients vanishing in recurrent neural network. It has an own memory which is capable to make forecast that is reliable reasonably. Hence, it's been utilised frequently in textual assessment, emotional analytics and identification of speech. Recently in extraction of polycyclic aromatic hydrocarbon, this method was utilised. Typically, in RNN, their exist one module for recurring and which has a structure of straight forward. In the tanh layer, four of LSTMs components work interactively and resemble as regular RNNs components. Three components of LSTM cell are output gate, input gate, and forget gate. The steps in the LSTM computation are as described in the following:

•The forget gate receives the value yields of the recent instant and values of present input time, which then calculated for producing the output result of forget gate's, as presented in the below equation:

$$F_g = \sigma(l_F.[p_{n-1}, y_n] + a_F) \qquad (2)$$

where, parameter range of F_g was (0,1), a_F is the forget gate's biases, l_F mass of forget gate's, p_{n-1} is the result of the most recent occurrence and y_n is the present time's input values.

•Input gates receives final output from the previous period and intake values of present time, that are calculated to

produce the values of yield and potential cell condition of intake gate, as indicated in the preceding equations:

$$I_g = \sigma(l_I.[p_{n-1}, y_n] + a_I) \qquad (3)$$

$$\grave{d}_n = \tanh(l_d.[p_{n-1}, y_n] + a_d) \qquad (4)$$

where, the l_I is input gate's mass, l_d is proposed input gate's value, a_I is input gate's biasing, and a_d is proposed input gate's biases, and I_g parameter ranges are (0,1).

•As mentioned below do change the present unit.

$$d_n = F_g * d_{n-1} + I_g * \grave{d}_n \qquad (5)$$

where, d_n's values fall possible in the limit (0, 1).

•At time n, p_{n-1} and y_n are received at output gates. Also, outcome O_g is defined as follows:

$$O_g = \sigma(l_O.[p_{n-1}, y_n] + a_O) \qquad (6)$$

where, a_O is biases of yield gate's, l_O is mass of output gate's, O_g's possible value is fall within limit (0, 1).

•The following equation illustrates the outcome computing of output nodes and LSTMs final output cell yield condition.

$$p_n = \tanh(d_n) * O_g \qquad (7)$$

4.4 Efficient fault diagnosis with CNN-LSTM fusion

A hybrid CNN-LSTM approach greatly improves squirrel cage induction motor fault detection. This technique combines LSTM's prowess in identifying temporal dependencies with CNN's capacity to extract spatial features from sensor data, including vibration, temperature, current, voltage, and acoustics. Prior to entering the model, raw sensor signals are preprocessed (noise filtered and normalized). A rich multimodal feature representation is produced by CNN layers identifying local patterns and LSTM layers learning time-based variations. Through differentiation from typical behavior, the trained model correctly classifies fault types, including misalignment, unbalance, and bearing damage. The model increases operational reliability, prolongs motor life, and reduces unscheduled downtime when integrated into a real-time monitoring system. The model's basic structure, which includes input layers, one-dimensional convolutional layers, pooling layers, LSTM hidden layers, and fully connected layers, is depicted in Figure 2.

5. RESULTS AND DISCUSSION

The study's conclusion was accomplished through the implementation of the suggested technique into practice with Python software with the intention of evaluating how well it worked for diagnosing motor faults. The findings of the study, which used performance metrics, conclusively show that the suggested method outperforms the already employed techniques in terms of accuracy and dependability. This accomplishment highlights the usefulness of the suggested method in improving the accuracy and effectiveness of motor fault diagnosis, making a significant contribution to the fields of industrial maintenance and machinery reliability.
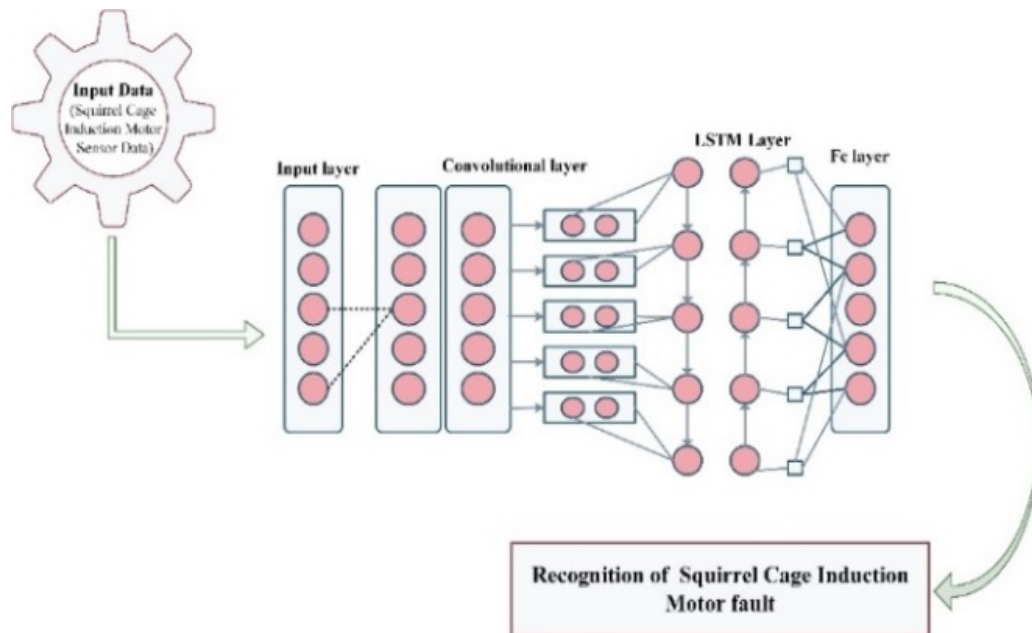
Figure 2. Architecture of the proposed hybrid deep learning model for motor fault diagnosis

5.1 Experimental outcome

Visualizing important characteristics of squirrel cage induction motors, such as vibration (represented as a time-series graph showing amplitude variations), temperature (represented as a line graph showing temperature fluctuations over time), current (represented similarly to temperature, with current values on the y-axis), acoustic data (typically visualised as a spectrogram revealing intensity across frequency ranges), and motor speed (plotted as a line graph showing RPM or Hz variation). These graphical depictions act as useful diagnostic tools, enabling engineers and operators to quickly spot anomalies, trends, or inconsistencies in motor behaviors. This enables prompt maintenance and ensures the dependability of industrial machinery.

The aforementioned charts would make it easier to comprehend how the counts of particular events or occurrences (such as vibrations, temperature spikes, current anomalies, acoustic events, speed variations, or voltage fluctuations) correlate with the associated parameter values. This could have implications for the health and performance of the motor system. Figure 3 displays a graph of the squirrel cage motor's count in relation to vibration, temperature, current, acoustic speed, and voltage.
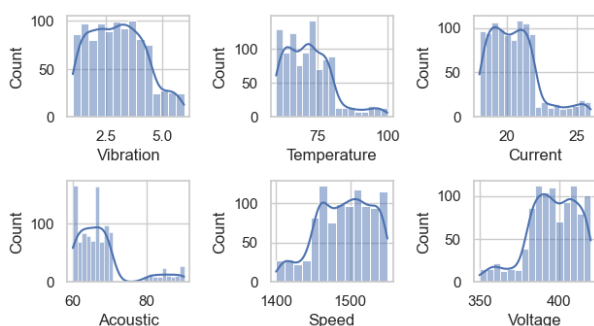
Figure 3. Graphical representation of vibration, temperature, current, acoustic, speed and voltage

5.1.1 Fault diagnosis assessment

Vibration, Temperature, Current, Acoustic, Speed, and Voltage are key metrics that must be thoroughly analysed and plotted against two different motor situations, "Normal" and "Fault." These representations are essential for assessing how well motor fault detection methods work. Engineers can identify anomalous vibration patterns that point to defects by visualising vibration data. Temperature charts reveal temperature changes and reveal overheating problems that are frequently linked to flaws. Electrical current changes are highlighted in current graphs, indicating probable motor abnormalities. Visualisations of acoustic intensity aid in the detection of anomalous noise patterns linked to problems. Speed charts show variations in motor rotation speed associated with different fault types. Visualising voltage data could illustrate voltage variations associated with motor problems. Figure 4 illustrates how graphical evaluations enable operators and maintenance staff to quickly identify and address motor defects, improving motor reliability, lowering downtime, and optimising industrial operations.

5.1.2 Heat map

In order to visualise the correlations among several variables, a heatmap could be helpful. Although humidity and condition are categorical or binary variables and do not lend themselves well to this type of graphical representation, it is crucial to highlight that they are not often represented in a heatmap. However, you can make a heatmap to see the connections between the other continuous variables in your dataset (such as vibration, temperature, current, acoustic speed, and voltage).

To see how different parameters of a squirrel cage induction motor interact with one another and correlate with one another, a heatmap is created. The variables are Motor Speed (in RPM or Hz), Acoustic Intensity (across frequency ranges), Vibration (measured in mm/s or g), Temperature (in degrees Celsius or Fahrenheit), Current (in amperes), and Voltage (in volts). Each heatmap cell indicates the correlation coefficient between two parameters, with the intensity and direction of the association denoted by a colour scale. Warm hues like red or orange denote positive correlations, indicating that the tendency is for the two parameters to rise together as one increase. In contrast, cool hues like blue signify negative

correlations, which suggests that as one parameter rises, the other tends to fall. Such a heatmap offers insights into potential cause-and-effect linkages and highlights areas of interest for additional research or investigation The Heatmap for the suggested technique is displayed in Figure 5.

5.1.3 Training accuracy and loss

The model's ability to correctly categorise cases in the training dataset is how well it performs in terms of failure identification for motors.

It calculates the percentage of both normal and problematic motor circumstances that the model is able to identify during training. A high training accuracy indicates that the model is effectively learning to distinguish between healthy and unhealthy motor behavior using the data at hand. However, high training accuracy by itself does not guarantee that the model will generalize well to novel motor scenarios or data, and over-fitting needs to be closely monitored. Training loss, sometimes expressed as a loss function or cost function, is the discrepancy between the model's predictions and the actual fault labels or conditions in the training dataset.

During training, the model iteratively adjusts its internal parameters to lessen this loss. For fault detection; the loss function calculates the difference between the actual motor state and the expected motor state, which can be either normal or defective.

In order to evaluate the development of your defect detection model during training, it is crucial to keep track of both training loss and accuracy. To evaluate how successfully the model generalises to novel, unforeseen motor circumstances or data, it is necessary to combine these measures with validation metrics, like loss validation and accuracy. Additionally, to guarantee the model's dependability and to identify potential problems like overfitting or underfitting, you should think about utilising approaches like cross-validation and monitoring learning curves. Figure 6 displays the suggested model's training accuracy and loss.
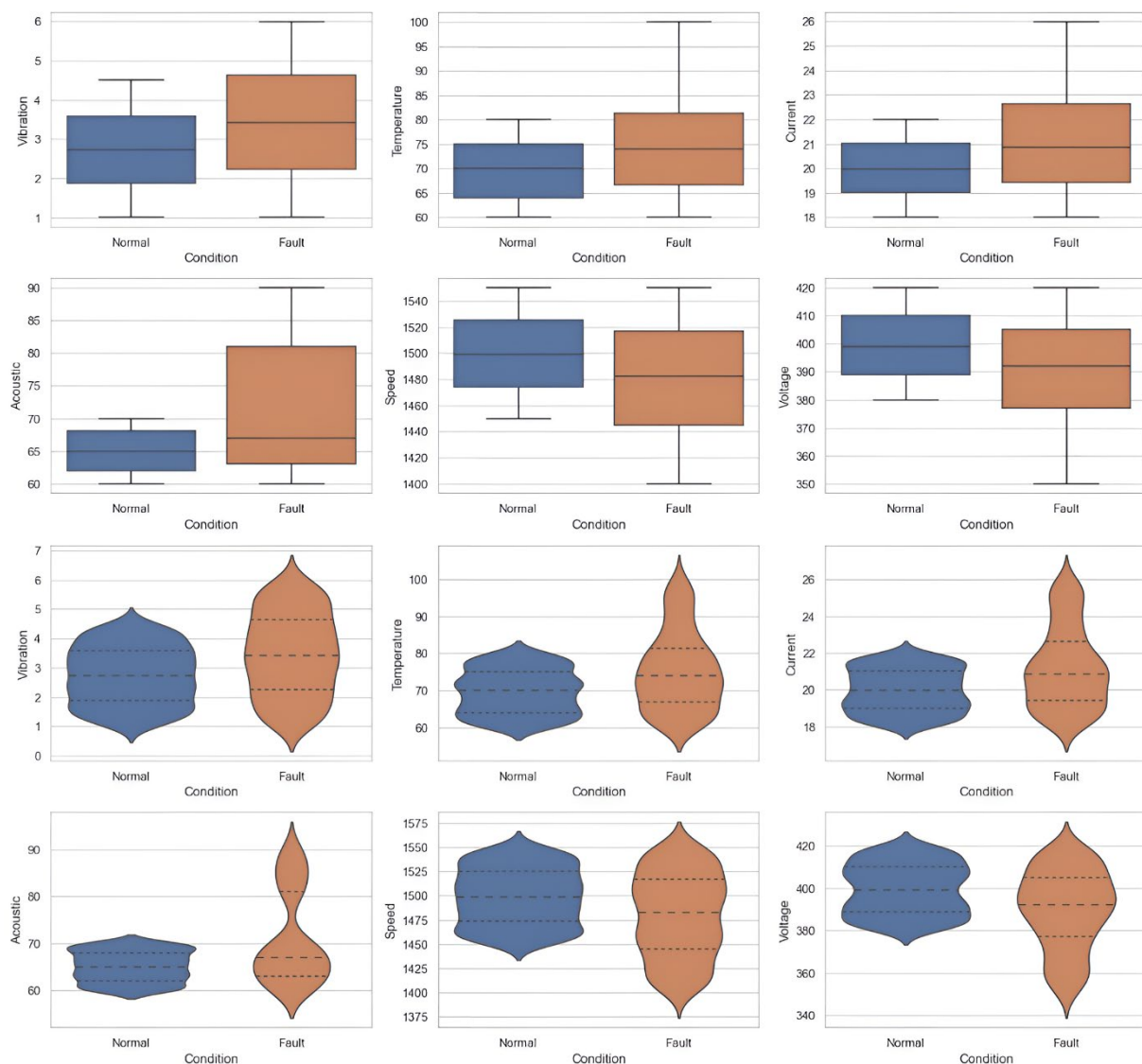
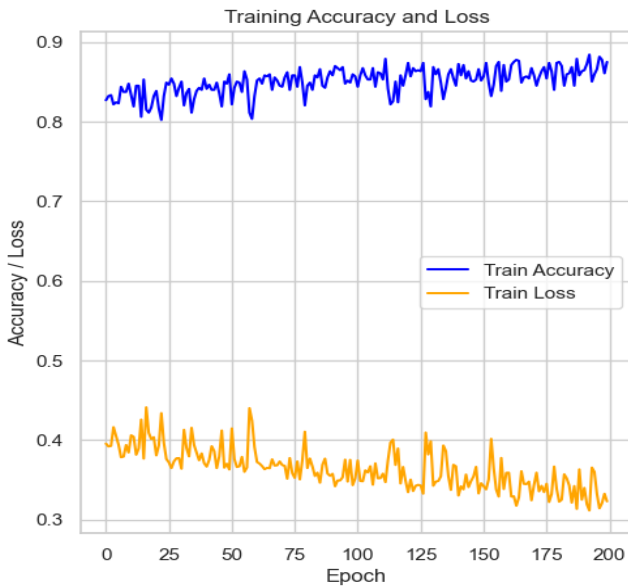**Figure 4.** Fault diagnosis in motor with different parameters
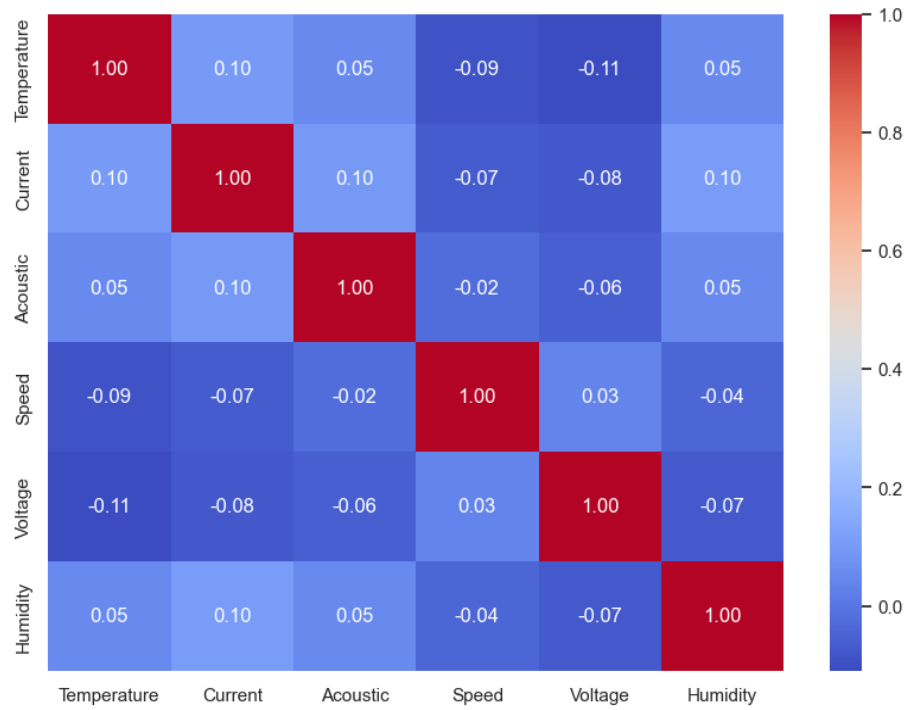
Figure 5. Heat map

A batch size of 32 was used to train the model and categorical cross-entropy loss over 200 epochs. To improve generalization and lessen overfitting, a five-fold cross-validation approach was employed. To maximize training efficiency, a dynamic learning rate scheduler and early stopping were used.
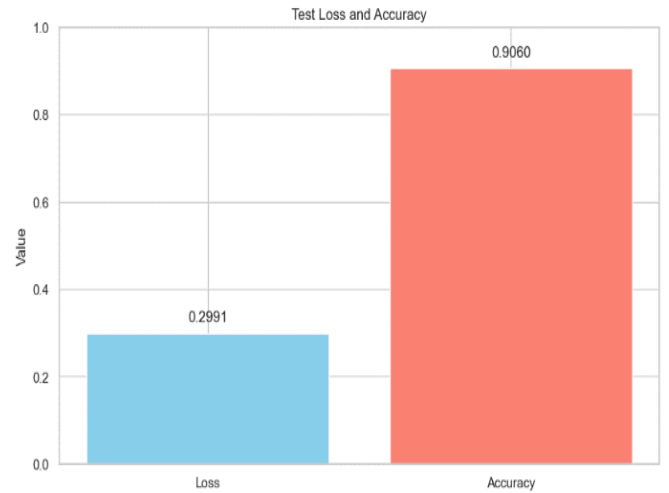

Figure 6. Training accuracy and loss

5.1.4 Testing accuracy and loss

The indicators for testing accuracy and testing loss in Table 3 combined imply that the fault detection model performs pretty well on the testing dataset. The model's predictions are typically close to the actual fault states, as shown by the comparatively low testing loss, and the model's high testing accuracy, which emphasises its skill in correctly recognising motor faults. These metrics offer insightful evaluations of the model's performance in practical fault detection applications.

Table 3. Testing accuracy and loss

Metric	Ratio (%)
Testing Loss	0.2991
Testing Accuracy	0.9060

Figure 7. Testing accuracy and loss

The testing loss, also known as the cost function or loss function, finds how well the trained defect detection model performs when generating predictions on an unrelated testing dataset. An average amount of error or disparity among model's predictions and the actual fault labels or circumstances in the testing dataset is indicated by a testing loss of 0.2991 in this case. Better model performance is often shown by lower testing loss values, which imply that predictions of model match closely the actual fault states in the testing data. The percentage of accurate predictions the fault detection model made when used on the testing dataset is represented by the testing accuracy. In this instance, a testing accuracy of 0.9060 denotes that roughly 90.60% of the occurrences in the testing

dataset had fault circumstances correctly detected by the model. The testing accuracy and loss ratio of the proposed approach are shown in Figure 7.

5.1.5 ROC curve

The complete evaluation of a binary classification model, particularly in the framework of defect detection in motors, is provided by the ROC (Receiver Operating Characteristic) curve and an Area Under the Curve (AUC) value of 0.91. The True Positive Rate (Sensitivity) vs the False Positive Rate (1-Specificity) of the ROC curve, which contrasts the model's ability to distinguish between healthy and unhealthy motor states across different categorization thresholds, graphically indicates how well the model performs in this regard. With a 91% chance of properly prioritising a randomly chosen defective motor above a healthy one, the model shows exceptional performance in this discriminating test, as indicated by its AUC of 0.91. This high AUC value highlights the model's durability and highlights its ability to draw solid conclusions, demonstrating its efficacy as a tool for motor failure identification when precision is crucial. The ROC Curve for the proposed approach is shown in Figure 8.
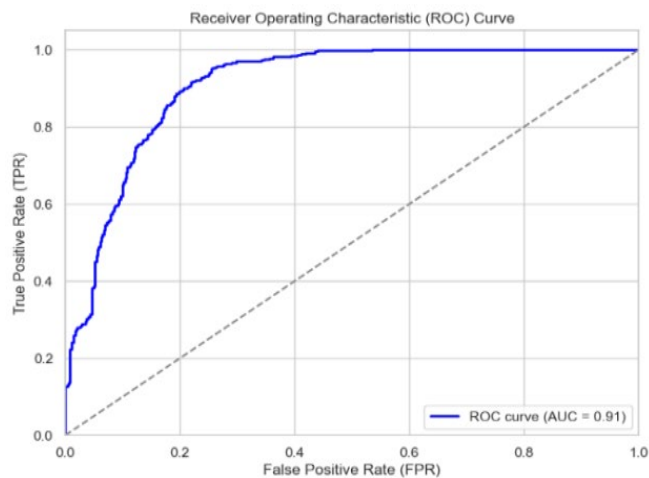

Figure 8. ROC-curve

5.1.6 Precision-Recall curve

Figure 9 shows a graphic representation of the Precision-Recall curve, which is employed to evaluate the effectiveness of a binary classification model, especially when working with unbalanced datasets or circumstances where one class is more important to identify than the other. As the classification threshold changes, Precision is plotted on the y-axis and Recall (Sensitivity) on the x-axis. Recall quantifies the model's capacity to properly identify every occurrence of a positive prediction, whereas Precision measures the accuracy of positive predictions. This curve demonstrates the trade-off between recall and precision as the classification threshold for the model changes. Precision measures how well the model can recognise motor defects, guaranteeing that when it forecasts a fault, it is very likely to be right. Recall, on the other hand, measures how well the model can detect all genuine motor defects while minimising false negatives.

The Precision-Recall curve offers a specific evaluation in situations like fault detection in motors, where the expense of failing to detect a fault (false negatives) or performing unneeded maintenance (false positives) might be significant. It offers insights on the model's ability to retain high precision while making sure that a sizable portion of genuine problems

is discovered (high recall) by focusing on precision-recall trade-offs. The performance of the model as a whole is quantified by the area under the Precision-Recall curve (AUC-PR), with higher values suggesting better precision-recall balances. A high AUC-PR indicates that the model can reliably identify motor defects in fault detection applications while minimizing expensive false alarms, making it a crucial tool for assuring motor dependability and operational efficiency.
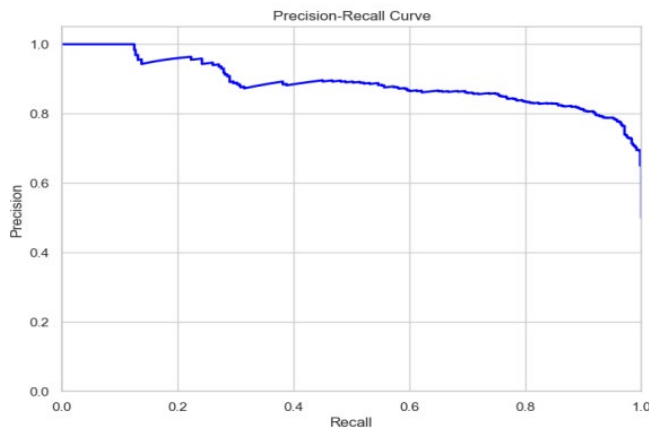

Figure 9. Precision-Recall curve

5.1.7 Confusion matrices

A more detailed assessment of misclassification patterns is made possible by the confusion matrix, which displays true positives, false positives, true negatives, and false negatives for every class as shown in Figure 10. This analysis facilitates additional model improvement by highlighting the fault categories that are most likely to cause confusion.
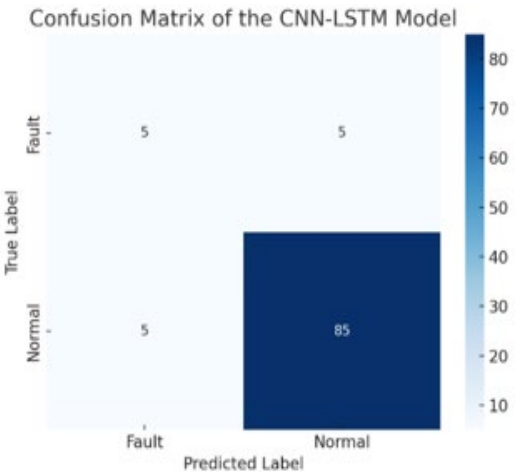

Figure 10. Confusion matrix showing CNN-LSTM model performance for normal and fault classification

The CNN-LSTM model's confusion matrix, which displays its classification performance under both normal and fault conditions, is shown here. It helps assess how well the model differentiates between normal operation and motor faults by providing a visual summary of the number of instances for each class that were correctly and incorrectly classified.

5.2 Effectiveness assessment of the proposed approach

Precision: Precision is defined as the proportion of

prediction correctly classified as belonging to a class to all prediction correctly classified as belonging to a class. Since it is sensitive to incorrect classification, precision is in fact a crucial factor in TC results. Additionally, incorrect categorisation produced less precise findings.

$$Percision = \frac{T^{positive}}{T^{positive} + F^{positive}} \qquad (8)$$

Recall: Recall is defined as the number of predictions that were correctly assigned to the class divided by the total number of predictions that actually belonged to the class.

$$Recall = \frac{T^{positive}}{T^{positive} + F^{Negative}} \qquad (9)$$

5.2.1 Accuracy comparison

The following Table 4 shows the accuracy obtained in based on four different methods. From the table it shows that the Proposed (CNN-LSTM) has the better accuracy than other three methods and the graphical representation of the comparison is shown in Figure 11.

Table 4. Accuracy comparison

Technique	Accuracy
CNN	88
MLP	81
SVM	78
LSTM	83
Proposed (CNN-LSTM)	90.6

In this comparative analysis of various techniques for a specific task, accuracy scores were measured for Convolutional Neural Networks (CNN) at 88%, Multilayer Perceptron (MLP) at 81%, Support Vector Machine (SVM) at 78%, Long Short-Term Memory (LSTM) at 83%, and a proposed approach combining CNN and LSTM (CNN-LSTM) outshining the others with an impressive accuracy rate of 90.6%. These findings show that, when compared to conventional machine learning techniques like MLP and SVM, as well as individual neural network architectures like CNN and LSTM, the proposed CNN-LSTM methodology outperforms in accuracy.
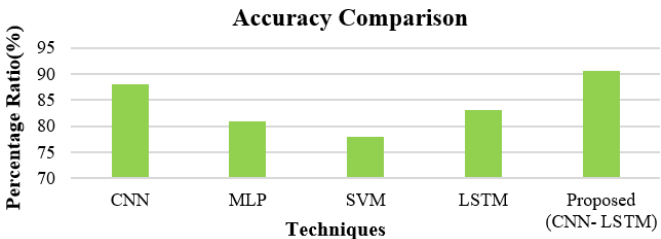
Figure 11. Accuracy comparison of the suggested approach

5.3 Discussion

The study demonstrates high fault diagnostic accuracy in industrial applications by integrating CNNs for spatial feature extraction and LSTM networks for temporal analysis. It identifies issues early, preventing downtime and equipment damage. Real-time monitoring and warning systems are included, ensuring maintenance team response. The study's generalizability and adaptability make it suitable for various

industrial configurations and squirrel cage induction motors.

6. CONCLUSION AND FUTURE WORK

The CNN-LSTM technique has been shown to be highly accurate and efficient in diagnosing faults in squirrel cage induction motors in industrial applications. It can distinguish between normal motor performance and various fault conditions, such as bearing wear, imbalance, and electrical problems. This high level of accuracy is crucial in industrial settings, where machinery reliability and effectiveness are crucial. The model's ability to integrate spatial and temporal analysis of sensor data is crucial for capturing subtle spatial patterns and complex temporal relationships within the motor's operational data. The CNN-LSTM model has the potential to increase industrial production and reduce costs when used in real-time motor condition monitoring systems. It can quickly identify anomalies, enable proactive maintenance procedures, and prevent unanticipated shutdowns. This proactive approach optimizes manufacturing procedures, protecting machinery and boosting overall productivity. Regular updates and retraining with fresh data are necessary to maintain the high accuracy of the CNN-LSTM model over time. This allows the model to adapt to changing operating conditions and motor behavior changes, maintaining its efficacy in fault diagnostics. In conclusion, the CNN-LSTM approach offers an effective and precise solution for defect diagnosis in industrial applications, with an accuracy of 90.6%.

Apart from the prediction accuracy of the model, its practical deployment factors were also taken into account. Because of its small size about 2.5 MB, the final CNN-LSTM model can be deployed on edge devices with limited resources. Real-time fault detection is made possible by an average inference time per sample of less than 50 milliseconds. Because of the model's small memory footprint and low computational complexity, it integrates seamlessly with edge computing systems, enabling on-site decision-making independent of constant cloud access. This improves responsiveness and lowers communication overhead, which makes the method ideal for industrial IoT settings where dependability and latency are crucial.

Future studies could explore the approach's ability to handle larger datasets and explore edge computing approaches to lower processing requirements. Field tests and case studies conducted in actual industrial settings would also confirm the effectiveness of this strategy in practice.

REFERENCES

[1] Doppelbauer, M. (2022). Institute-History-The invention of the electric motor 1856-1893. https://www.eti.kit.edu/english/1390.php.

[2] Electrical 4U. Squirrel Cage Induction Motor: Working Principle & Applications. https://www.electrical4u.com/squirrel-cage-induction-motor/.

[3] Asad, B., Vaimann, T., Belahcen, A., Kallaste, A., Rassõlkin, A., Iqbal, M.N. (2020). The cluster computation-based hybrid FEM–Analytical model of induction motor for fault diagnostics. Applied Sciences, 10(21): 7572. https://doi.org/10.3390/app10217572

[4] Alam, M.A., Kumar, R., Yadav, A.S., Arya, R.K., Singh,

V.P. (2023). Recent developments trends in HVAC (heating, ventilation, and air-conditioning) systems: A comprehensive review. Materials Today: Proceedings. https://doi.org/10.1016/j.matpr.2023.01.357

[5] Kumar, R.R., Andriollo, M., Cirrincione, G., Cirrincione, M., Tortella, A. (2022). A comprehensive review of conventional and intelligence-based approaches for the fault diagnosis and condition monitoring of induction motors. Energies, 15(23): 8938. https://doi.org/10.3390/en15238938

[6] Deng, L. (2014). A tutorial survey of architectures, algorithms, and applications for deep learning. APSIPA Transactions on Signal and Information Processing, 3: e2.

[7] Szegedy, C., Vanhoucke, V., Ioffe, S., Shlens, J., Wojna, Z. (2016). Rethinking the inception architecture for computer vision. In Proceedings of the IEEE Conference on Computer Vision and Pattern Recognition, Salt Lake City, UT, USA, pp. 2818-2826.

[8] He, M., He, D. (2017). Deep learning based approach for bearing fault diagnosis. IEEE Transactions on Industry Applications, 53(3): 3057-3065. https://doi.org/10.1109/TIA.2017.2661250

[9] Ince, T., Kiranyaz, S., Eren, L., Askar, M., Gabbouj, M. (2016). Real-time motor fault detection by 1-D convolutional neural networks. IEEE Transactions on Industrial Electronics, 63(11): 7067-7075. https://doi.org/10.1109/TIE.2016.2582729

[10] Verstraete, D., Ferrada, A., Droguett, E.L., Meruane, V., Modarres, M. (2017). Deep learning enabled fault diagnosis using time-frequency image analysis of rolling element bearings. Shock and Vibration, 2017(1): 5067651. https://doi.org/10.1155/2017/5067651

[11] Lee, J.H., Pack, J.H., Lee, I.S. (2019). Fault diagnosis of induction motor using convolutional neural network. Applied Sciences, 9(15): 2950. https://doi.org/10.3390/app9152950

[12] Zhu, D., Zhang, Y., Zhao, L. (2019). Fault diagnosis method for rolling element bearing with variable rotating speed using envelope order spectrum and convolutional neural network. Journal of Intelligent & Fuzzy Systems, 37(2): 3027-3040. https://doi.org/10.3233/JIFS-190101

[13] Pandarakone, S.E., Masuko, M., Mizuno, Y., Nakamura, H. (2018). Deep neural network based bearing fault diagnosis of induction motor using fast Fourier transform analysis. In 2018 IEEE energy conversion congress and exposition (ECCE), Portland, OR, USA, pp. 3214-3221. https://doi.org/10.1109/ECCE.2018.8557651

[14] Hsueh, Y.M., Ittangihal, V.R., Wu, W.B., Chang, H.C., Kuo, C.C. (2019). Fault diagnosis system for induction motors by CNN using empirical wavelet transform. Symmetry, 11(10): 1212. https://doi.org/10.3390/sym11101212

[15] Li, S., Liu, G., Tang, X., Lu, J., Hu, J. (2017). An ensemble deep convolutional neural network model with improved DS evidence fusion for bearing fault diagnosis. Sensors, 17(8): 1729. https://doi.org/10.3390/s17081729

[16] Wang, L.H., Zhao, X.P., Wu, J.X., Xie, Y.Y., Zhang, Y.H. (2017). Motor fault diagnosis based on short-time Fourier transform and convolutional neural network. Chinese Journal of Mechanical Engineering, 30(6): 1357-1368. https://doi.org/10.1007/s10033-017-0190-5

[17] Wang, S., Xiang, J., Zhong, Y., Zhou, Y. (2018). Convolutional neural network-based hidden Markov models for rolling element bearing fault identification. Knowledge-Based Systems, 144: 65-76. https://doi.org/10.1016/j.knosys.2017.12.027

[18] Lu, C., Wang, Z., Zhou, B. (2017). Intelligent fault diagnosis of rolling bearing using hierarchical convolutional network based health state classification. Advanced Engineering Informatics, 32: 139-151. https://doi.org/10.1016/j.aei.2017.02.005

[19] Guo, X., Chen, L., Shen, C. (2016). Hierarchical adaptive deep convolution neural network and its application to bearing fault diagnosis. Measurement, 93: 490-502. https://doi.org/10.1016/j.measurement.2016.07.054

[20] Zhang, W., Li, C., Peng, G., Chen, Y., Zhang, Z. (2018). A deep convolutional neural network with new training methods for bearing fault diagnosis under noisy environment and different working load. Mechanical Systems and Signal Processing, 100: 439-453. https://doi.org/10.1016/j.ymssp.2017.06.022

[21] Wu, Y., Jiang, B., Wang, Y. (2020). Incipient winding fault detection and diagnosis for squirrel-cage induction motors equipped on CRH trains. ISA Transactions, 99: 488-495. https://doi.org/10.1016/j.isatra.2019.09.020

[22] Zhou, Y., Shang, Q., Guan, C. (2023). Three-phase asynchronous motor fault diagnosis using attention mechanism and hybrid CNN-MLP by multi-sensor information. IEEE Access, 11: 98402-98414. https://doi.org/10.1109/ACCESS.2023.3307770

[23] Toma, R.N., Prosvirin, A.E., Kim, J.M. (2020). Bearing fault diagnosis of induction motors using a genetic algorithm and machine learning classifiers. Sensors, 20(7): 1884. https://doi.org/10.3390/s20071884

[24] Pietrzak, P., Wolkiewicz, M. (2023). Demagnetization fault diagnosis of permanent magnet synchronous motors based on stator current signal processing and machine learning algorithms. Sensors, 23(4): 1757. https://doi.org/10.3390/s23041757

[25] El-Dalahmeh, M.D., Al-Greer, M., Bashir, I., El-Dalahmeh, M.A., Demirel, A., Keysan, O. (2023). Autonomous fault detection and diagnosis for permanent magnet synchronous motors using combined variational mode decomposition, the Hilbert-Huang transform, and a convolutional neural network. Computers and Electrical Engineering, 110: 108894. https://doi.org/10.1016/j.compeleceng.2023.108894

[26] Wang, C.S., Kao, I.H., Perng, J.W. (2021). Fault diagnosis and fault frequency determination of permanent magnet synchronous motor based on deep learning. Sensors, 21(11): 3608. https://doi.org/10.3390/s21113608

[27] Marfoli, A., Di Nardo, M., Degano, M., Gerada, C., Chen, W. (2020). Rotor design optimization of squirrel cage induction motor-part I: Problem statement. IEEE Transactions on Energy Conversion, 36(2): 1271-1279. https://doi.org/10.1109/TEC.2020.3019934

[28] Okwuosa, C.N., Akpudo, U.E., Hur, J.W. (2022). A cost-efficient MCSA-based fault diagnostic framework for SCIM at low-load conditions. Algorithms, 15(6): 212. https://doi.org/10.3390/a15060212

[29] Kim, B.S., Kim, T.G. (2019). Cooperation of simulation and data model for performance analysis of complex systems. International Journal of Simulation Modelling, 18(4): 608-619.

[30] Qin, L., Yu, N., Zhao, D. (2018). Applying the convolutional neural network deep learning technology

to behavioural recognition in intelligent video. Tehnički Vjesnik, 25(2): 528-535. https://doi.org/10.17559/TV-

20171229024444